EVOLUTION & DEVELOPMENT 12:6, 552–567 (2010)
DOI: 10.1111/j.1525-142X.2010.00441.x

Phylogeny informs ontogeny: a proposed common theme in the arterial pole of the vertebrate heart

Adrian C. Grimes,[a,*] Ana Carmen Durán,[b] Valentín Sans-Coma,[b] Danyal Hami,[c] Massimo M. Santoro,[d,e] and Miguel Torres[a]

[a]Departamento de Biología del Desarrollo Cardiovascular, Centro Nacional de Investigaciones Cardiovasculares Carlos III (CNIC), Melchor Fernández Almagro 3, 28029 Madrid, Spain
[b]Department of Animal Biology, Faculty of Science, University of Málaga, 29071 Málaga, Spain
[c]Duke University Medical Center, Department of Pediatrics (Neonatology), Research Drive—Jones Building, Durham, NC 27710, USA
[d]Molecular Biotechnology Center, University of Torino, Via Nizza 52, 10126 Torino, Italy
[e]Department of Enviromental and Life Science, University of Piemonte Orientale "A. Avogadro," Via Teresa Michel 11 I-15100 Alessadria, Italy
*Author for correspondence (email: acgrimes@cnic.es)

SUMMARY In chick and mouse embryogenesis, a population of cells described as the secondary heart field (SHF) adds both myocardium and smooth muscle to the developing cardiac outflow tract (OFT). Following this addition, at approximately HH stage 22 in chick embryos, for example, the SHF can be identified architecturally by an overlapping seam at the arterial pole, where beating myocardium forms a junction with the smooth muscle of the arterial system. Previously, using either immunohistochemistry or nitric oxide indicators such as diaminofluorescein 2-diacetate, we have shown that a similar overlapping architecture also exists in the arterial pole of zebrafish and some shark species. However, although recent work suggests that development of the zebrafish OFT may also proceed by addition of a SHF-like population of cells, the presence of a true SHF in zebrafish and in many other developmental biological models remains an open question. We performed a comprehensive morphological study of the OFT of a wide range of vertebrates. Our data suggest that all vertebrates possess three fundamental OFT components: a proximal myocardial component, a distal smooth muscle component, and a middle component that contains overlapping myocardium and smooth muscle surrounding and supporting the outflow valves. Because the middle OFT component of avians and mammals is derived from the SHF, our observations suggest that a SHF may be an evolutionarily conserved theme in vertebrate embryogenesis.

INTRODUCTION

Partly as a result of historical inconsistencies of terminology (Laane 1973a, b,c, d), there is considerable confusion over the outflow tract (OFT) of the vertebrate heart. This is based not only on the descriptions of its component parts, but also on the processes that guide its development. Another contributory factor is the extraordinary variety of heart morphologies that exist among even a limited number of comparative biological models, and the fact that some of the component structures of the OFT are developmentally transient in some species and can undergo exquisitely complex morphological changes during embryogenesis. For example, in avian and mammalian development, the early embryonic OFT, or "common outflow," is often described as consisting of two myocardial components, the proximal conus arteriosus and the distal truncus arteriosus. The entire outflow structure is occasionally called the conotruncus (e.g., Thompson et al. 1985; Bartelings and Gittenberger-de Groot 1989). The individual components, separated by a characteristic "bayonet bend" (Orts-Llorca et al. 1982) or "dog-leg bend" (Webb et al. 2003), are not easily identifiable, other than in chick embryos, and undergo complex remodelling processes throughout development, by which at least the proximal component, the conus arteriosus, is ultimately incorporated into the ventricles as the aortic vestibule and pulmonary infundibulum (Kirby and Waldo 1995). In contrast, in the chondrichthyans (sharks, skates, and rays), whereas there is an embryonic conus arteriosus that may be homologous to the common outflow of the avian and mammalian embryo (see Romer and Parsons 1986; Holmes 2005; Moorman et al. 2007), this structure persists into adulthood and is never incorporated into the ventricle. On the other hand, although similarly a homologous conus arteriosus undoubtedly exists in

the embryonic heart of at least the vast majority of apical teleosts (see Schib et al. 2002; Guerrero et al. 2004; Grimes et al. 2006; Icardo 2006; Grimes and Kirby 2009), the fact that it regresses toward and, in most cases, appears to be incorporated into the ventricle later in development means that it is not obvious in adult forms, except under careful histological scrutiny (see Grimes et al. 2006; Icardo 2006). This has resulted in the structure being described as merely vestigial or even missing entirely in many descriptions of the teleost heart (e.g., Satchell 1991; Farrell and Jones 1992).

More confusion in OFT nomenclature results from the same terms occasionally being used to describe structures with no obvious homology. So, from the examples above, should the conus arteriosus of chondrichthyans and birds be considered homologous structures, even though the former persists into adulthood, whereas the latter is incorporated into the ventricles during development? Or is the bulbus arteriosus described in frog species such as *Xenopus laevis* (e.g., Sedmera et al. 2003) an homologue of the zebrafish bulbus arteriosus, even though the former contains myocardium in its walls, whereas the latter lacks it?

Such issues are perpetuated by the suggestion that the term conus arteriosus should only be used to describe the region of the adult myocardial OFT that is derived from the embryonic "bulbus cordis" (Goodrich 1930). This introduces another term for which the only appropriate usage may be in reference to the early-stage mammalian OFT, where it generally identifies a region of the embryonic heart tube that will give rise to the right ventricle, conus arteriosus and truncus arteriosus. Unfortunately, the term's wide misuse along with differing descriptions of its component structures have led to considerable ambiguity (see Anderson et al. 1978). Moreover, while the term may not necessarily apply in the mammalian heart, it is certainly not applicable in the fishes. The term bulbus cordis has been used to describe the smooth muscle structure (the bulbus arteriosus) cranial to the teleost heart (e.g., Ekström and Korf 1986; Zhang et al. 2001) and the myocardial outflow of the lungfishes (e.g., Burggren and Johansen 1986) and of amphibians such as *Xenopus* (e.g., Horb and Thomsen 1999; Blitz et al. 2006). In fish embryogenesis, however, there is no myocardial structure that ever gives rise to a right ventricle, as the early fish heart tube gives rise to a single ventricle, and no other myocardial bulb-like structure is observed. Generally, later in development, the smooth muscle bulbus arteriosus develops beyond the cranial myocardial limit. In the chondrichthyans, the coelacanth, the lungfishes and some other basal actinopterygians such as the sturgeons, a prominent myocardial conus arteriosus persists to a greater or lesser degree into adulthood, but does not arise from anything akin to the mammalian bulbus cordis. Evolutionarily, because early air-breathing vertebrates undoubtedly had a requirement for additional myocardium that would allow the increasingly septated ventricle to become more substantial, particularly at the right side, it has been proposed that the intussuscepted conus provided at least some of that tissue (e.g., Romer and Parsons 1986; Holmes 2005; Moorman et al. 2007). Therefore, in ontogeny the (mammalian) conus arteriosus may be described as being derived from Goodrich's definition of the bulbus cordis, but in phylogenetic terms it is likely that the bulbus cordis is derived from the conus arteriosus (see Grimes and Kirby 2009).

In an attempt to address some of these issues, using histological and immunohistochemical approaches, we undertook a comprehensive study of the OFT of a wide range of vertebrate species, from the chondrichthyans, through basal actinopterygian and apical teleost fishes, to land-based tetrapods, including amphibian, reptilian, avian, and mammalian species. We find in all species examined that there are three fundamental components of the cardiac OFT: a proximal, myocardial component that extends from the ventricular outflow to the base of the outflow valves; a distal, smooth muscle component that extends from the cranial limit of the myocardial component to the wall of the pericardial cavity; and a middle component that surrounds and supports the outflow valves. Depending on the species and on developmental stage, this middle component contains varying proportions of both myocardium and smooth muscle that form an overlapping seam between the proximal, myocardial, and distal, smooth muscle components. Coincident with the smooth muscle in the middle and distal components are abundant elastic fibers. We propose that these three distinct components are ubiquitous among vertebrates and suggestive of evolutionary conservation in the developmental program of the OFT. Further, we suggest a simple nomenclature for the OFT that would be applicable across all species and which would therefore reduce much of the confusion that pervades the literature.

MATERIALS AND METHODS

Specimen acquisition

Unless otherwise stated, all hearts were dissected from the specimens, fixed overnight at 4°C, in either 4% paraformaldehyde (PFA) or Dent's fixative (4:1 methanol:dimethyl sulfoxide) or MAW (2:2:1 methanol:acetone:water). After fixation, specimens were dehydrated into methanol (MeOH) and stored at −20°C until required for histological and immunohistochemical processing.

Adult wild-type zebrafish (*Danio rerio*) were collected from the zebrafish housing facility at the Centro Nacional de Investigaciones Cardiovasculares Carlos III (CNIC), Madrid, Spain. They were anaesthetized in 0.016% tricaine before fixation.

Five late-juvenile (4–5 years old) Australian lungfish (*Neoceratodus forsteri*), a kind gift of Professor Jean Joss, were obtained from the breeding ponds at the Department of Biological Sciences, Macquarie University, Sydney, Australia. The animals were sacrificed and the hearts dissected on site. After fixation and dehydration, the hearts were shipped to Spain and, upon arrival, transferred to fresh 100% MeOH for storage at −20°C until required.

The hearts from two late juvenile (2 years old) sturgeon (*Acipenser naccarii*) were excised on site at the Sierra Nevada Fishery at Riofrío, Granada, Spain, fixed in 4% PFA at ambient temperature for 24 h and transferred into 100% MeOH for transportation to CNIC. Upon arrival, the hearts were transferred to fresh 100% MeOH and stored at −20°C until required.

Various teleost and chondrichthyan species were collected in the western Mediterranean by scientific vessels belonging to the Spanish Institute of Oceanography. After species identification, the hearts were excised and fixed in either 4% PFA or MAW for varying lengths of time dependent upon the day of capture. Upon return to shore, the hearts were transferred into fresh fixative and stored at 4°C for transfer to CNIC in Madrid. Upon arrival, the hearts were dehydrated into MeOH and stored at −20°C until required.

The hearts of four adult *Xenopus tropicalis*, a kind gift of Dr. José Luis Gómez-Skarmeta, Centro Andaluz de Biología del Desarrollo CSIC/Universidad Pablo de Olavide, Sevilla, Spain, were excised, fixed in 4% PFA, dehydrated into MeOH, and shipped to CNIC on ice. Upon arrival, the hearts were transferred to fresh 100% MeOH and stored at −20°C until required.

The hearts of northern walleye (*Sander vitreus*), pinfish (*Lagodon rhomboides*), white bass (*Morone chrysops*), largemouth bass (*Micropterus salmoides*), Atlantic flounder (*Paralichthys dentatis*), and silverside (*Menidia menidia*) were collected during fishing trips in the continental USA (courtesy of Kyle Erwin, Durham, NC and Daniel Gefroh, Underwood, ND). Hearts were excised on site and fixed in 4% PFA or Dents fixative on ice for 24 h and transferred into 100% MeOH for transportation to Duke University. Upon arrival, the hearts were transferred to fresh 100% MeOH, stored at −20°C until required and then processed for paraffin embedding and sectioning.

Five young-of-year (2002) bowfin (*Amia calva*) were acquired from Drs. Jan J. Hoover and Steven G. George at the US Army Corps of Engineers Environmental Laboratory, Vicksburgh, Mississippi. Also, six each young-of-year specimens of the American paddlefish (*Polyodon spathula*) and the shovelnose sturgeon (*Scaphirhynchus platorynchus*) were acquired from Drs. James E. Garvey and Sara Tripp at the Fisheries and Illinois Aquaculture Center, Southern Illinois University, Carbondale, Illinois. All specimens had been fixed in formalin and stored in ethanol.

Adult and embryonic mouse, chicken, and duck heart sections were acquired from researchers at CNIC when such sections were surplus to requirement. Previously, these specimens had been fixed in 4% PFA, dehydrated in methanol series, cleared in xylenes, and embedded in paraffin.

All other species listed in Table 1 and not specifically mentioned previously were acquired from various European tropical fish and pet wholesale outlets or local fish markets in the Madrid area (Spain) and processed similarly.

Paraffin embedding and sectioning

Following whole-mount imaging, hearts were transferred from 100% MeOH into xylenes and allowed to equilibrate for 5 min before being placed in paraffin at 60°C. Hearts were embedded in disposable plastic molds and allowed to cool before being sectioned in transverse, sagittal, or longitudinal orientation at 8 μm on a Leica RM2155 microtome (Leica, Wetzlar, Germany), mounted on glass sides and allowed to dry overnight. Slides were heated to 60°C in an oven, placed in xylenes for 5 min, rehydrated through ethanol series to water, and prepared for histological or immunohistochemical processing.

Histological techniques for light microscopy

After hydration, sections of the heart were stained with haematoxylin-eosin for general assessment of tissue structure or with a commercially available elastic trichrome stain (Sigma, Madrid, Spain) to highlight elastic fibers and collagen.

Immunohistochemistry

After hydration, sections were treated for appropriate antigen retrieval by either predigestion with 0.05% trypsin (Sigma) in 0.1% calcium chloride at 37°C for 15 min or by boiling the slides in sodium citrate buffer (10 mM sodium citrate/0.5% Tween 20 pH6.0) for 20 min in a microwave and allowing them to cool in the buffer left at room temperature for a further 20 min. Following antigen retrieval, sections were rinsed in Tris/Tween/DMSO (0.1 M Tris [pH 7.6]/0.1% Tween/2% DMSO) and preblocked in blocking buffer (Tris/Tween/DMSO containing 2% normal goat serum and 1% bovine serum albumin). For smooth muscle labeling, sections were incubated for 1 h each in blocking buffer containing either 1:300 anti-smooth muscle α-actin monoclonal antibody (clone IA4, Sigma) or 1:500 anti-smooth muscle myosin light chain kinase monoclonal antibody (clone K36, Sigma) or 1:200 anti-SM22α polyclonal antibody (AbCam, Cambridge, UK) or 1:250 anti-zebrafish transgelin (SM22α) polyclonal antibody (Santoro et al. 2009), followed by 1:200 AlexaFluor 488 secondary antibodies (Molecular Probes, Eugene, OR, USA) of the appropriate species and isotype. For myocardial labeling, sections were serially incubated for 1 h each with 1:20 monoclonal antibody MF20 supernatant or 1:20 monoclonal antibody CH1 supernatant (both from Developmental Studies Hybridoma Bank, University of Iowa, IA, USA) and 1:200 AlexaFluor 594 goat anti-mouse IgG_{2b} or IgG_1 secondary antibody (Molecular Probes) in blocking buffer. Between each incubation, slides were rinsed 2 × 5 min in Tris/Tween/DMSO and reblocked in blocking buffer for 5 min. In each case, as a control, similar sections were incubated with secondary antibodies only. Following labeling, sections were rinsed in water and coverslipped using ProLong Gold Antifade Reagent with DAPI (Invitrogen, Barcelona, Spain).

Imaging

Various microscopes were utilized for imaging sections as follows:

Nikon A1R inverted confocal microscope (Nikon, Dusseldorf, Germany) using either a PlanApo 10 × /0.45 or VC 20 × /0.75 objective and 405, 488, and 594 nm to excite DAPI, AlexaFluor488 and AlexaFluor594, respectively. Images were acquired using a built-in automated tile scan routine and NIS-Elements software suite.

Nikon Eclipse 90*i* Advanced Motorized Advanced Research Microscope fitted with Nikon DXM1200C digital color camera and fluorescence source. Images were acquired using the Nikon ACT-1 software package (Version 2.63).

Leica MZ16FA motorized fluorescence stereomicroscope with × 2 planapochromatic objective and Leica DFC310FX digital color camera. Acquisition was by the Leica software application suite (LAS).

After acquisition, images were compiled using Adobe Photoshop.

Table 1. Species investigated in this study

Order	Family	Species	Common name
Rodentia	Muridae	*Mus musculus*	House mouse
Galliformes	Phasianidae	*Gallus gallus*	Chicken
Anseriformes	Anatidae	*Anas undulatus*	Yellow-billed duck
Squamata	Polychrotidae	*Anolis carolinensis*	Green anole
Anura	Pipidae	*Xenopus laevis*	African clawed frog
Ceratodontiformes	Ceratodontidae	*Neoceratodus forsteri*	Australian lungfish
Lepidosireniformes	Lepidosirenidae	*Lepidosiren paradoxa*	African (slender) lungfish
	Protopteridae	*Protopterus dolloi*	South American lungfish
Polypteriformes	Polypteridae	*Polypterus ornatipinnis*	Ornate bichir
		Polypterus senegalus	Gray bichir
Acipenseriformes	Acipenseridae	*Acipenser baerii*	Siberian sturgeon
		Acipenser stellatus	Stellate sturgeon
		Acipenser naccarii	Adriatic sturgeon
		Scaphirhynchus platorynchus	Shovelnose sturgeon
	Polyodontidae	*Polyodon spathula*	American paddlefish
Amiiformes	Amiidae	*Amia calva*	Bowfin
Lepisosteiformes	Lepisosteidae	*Lepisosteus osseus*	Longnosed gar
Osteoglossiformes	Osteoglossidae	*Osteoglossum bicirrhosum*	Arowana
Cypriniformes	Cyprinidae	*Danio rerio*	Zebrafish
Characiformes	Ctenoluciidae	*Ctenolucius hujeta*	Gar characin
Gymnotiformes	Apteronotidae	*Apteronotus albifrons*	Black ghost knifefish
Siluriformes	Loricaniidae	*Hypostomus plecostomus*	Suckermouth catfish
Clupeiformes	Clupeidae	*Sardina pilchardus*	European pilchard
Salmoniformes	Salmonidae	*Salmo trutta*	Sea trout
Atheriniformes	Atherinopsidae	*Menidia menidia*	Atlantic silverside
Cyprinodontiformes	Poeciliidae	*Xiphophorus hellerii*	Green swordtail
Perciformes	Channidae	*Channa micropeltes*	Giant snakehead
	Coryphaenidae	*Coryphaena hippurus*	Dolphinfish
	Moronidae	*Dicentrarchus labrax*	European seabass
		Morone chrysops	White bass
		Morone americana	White perch
	Sparidae	*Sparus aurata*	Gilthead seabream
		Lagodon rhomboides	Pinfish
	Percidae	*Sander vitreus*	Walleye
	Centrarchidae	*Micropterus salmoides*	Largemouth bass
	Scombridae	*Scomber scombrus*	Atlantic mackerel
		Katsuwonus pelamis	Skipjack tuna
Pleuronectiformes	Paralichthyidae	*Paralichthys dentatus*	Summer flounder
Carcharhiniformes	Scyliorhinidae	*Scyliorhinus canicula*	Small-spotted catshark
		Galeus melastomus	Blackmouth catshark
		Galeus atlanticus	Atlantic sawtail catshark
Squaliformes	Etmopteridae	*Etmopterus spinax*	Velvet-belly lantern shark
	Dalatidae	*Dalatias licha*	Kitefin shark
	Oxynotidae	*Oxynotus centrina*	Angular roughshark
Torpediniformes	Torpedinidae	*Torpedo marmorata*	Marbled electric ray
		Torpedo nobiliana	Atlantic torpedo
Rajiformes	Rajidae	*Leucoraja naevus*	Cuckoo ray
Chimaeriformes	Chimaeridae	*Chimaera monstrosa*	Ratfish

RESULTS

Conserved markers of myocardium and smooth muscle label the OFT of many vertebrates

Using immunohistochemical markers, we have found evidence for high levels of conservation in the structural proteins present in vertebrate cardiac and smooth muscle. MF20 (a monoclonal antibody raised against chicken gizzard sarcomeric myosin) and CH1 (a monoclonal antibody raised against chicken cardiac muscle tropomyosin) both bind with high affinity to the cardiomyocytes of many species of chondrichthyan, teleost, amphibian, reptile, avian, and mammal.

Fig. 1. Architectural homology in the arterial pole of two widely diverged species. In all three images, cranial is to the top. (A) Detail of the chick pulmonary outflow, gestational day 11, sectioned longitudinally and labeled with MF20 (myocardium—red) and anti-SMA (smooth muscle—green). The pulmonary outflow valves are surrounded and supported by a collar of myocardium. Smooth muscle known to be derived from the secondary heart field (SHF) can be seen at the lumenal face of the myocardial collar, extending caudally from the base of the arterial trunk to the level of the valves (arrowheads). Arrows show distal outflow tract smooth muscle known to be neural crest derived. The smooth muscle in the remnant of the aorticopulmonary septum (aps) is also neural crest derived. PI, pulmonary infundibulum; PT, pulmonary trunk. Scale bar = 250 μm (image adapted from Waldo et al. 2005). (B) Detail of the adult zebrafish arterial pole sectioned longitudinally and labeled with MF-20 (red) and anti-MLCK (smooth muscle—green). DAPI (blue) labels nuclei. White arrowheads show that, as in the chick, the valves are supported by a collar of myocardium (the conus arteriosus) and that smooth muscle extends caudally from the base of the bulbus arteriosus (BA) to the level of the valve leaflets. Scale bar = 100 μm. (C) Similar longitudinal section of adult zebrafish stained with elastic trichrome, showing an abundance of fibrous and elastic proteins (arrowheads) in the "fibrous ring" connecting the ventricle (V) with the bulbus arteriosus (BA). Scale bar = 100 μm.

Similarly, the monoclonal antibodies anti-SMA (raised against an N-terminal synthetic decapeptide of smooth muscle α-actin) and anti-MLCK (raised against chicken gizzard myosin light chain kinase), and two rabbit polyclonal antibodies for SM22α, an early marker of differentiated smooth muscle (raised against synthetic peptides derived from mouse SM22α and zebrafish transgelin, respectively) are cross-reactive with the smooth muscle present in the vasculature and OFT of many vertebrates. This conservation allowed us to examine the OFT of a wide range of species in fine detail. We found that the most effective protocol for labeling the OFT or the widest range of species was fixation with a precipitating fixative such as Dent's or MAW, antigen retrieval on rehydrated sections by boiling in sodium citrate buffer, and labeling using CH1 and anti-SM22α primary antibodies for myocardium and smooth muscle, respectively (see "Materials and methods" for details). Note that the SM22α antibodies also labeled distinct but limited subpopulations of myocardial cells in some species. These data are discussed where appropriate below. Table 1 shows the range of species used in this study.

Histology and immunohistochemistry reveal a conserved arterial pole architecture

This study was undertaken after our observation of a myocardial-smooth muscle overlap in the arterial pole of two evolutionarily widely diverged species, the chick and zebrafish (Fig. 1, A and B). Although these preliminary data were discussed briefly in Grimes and Kirby (2009), such a morphological feature is not widely reported in the literature but is suggestive of conservation in the developmental program that guides arterial pole ontogeny. In both chick and zebrafish, the smooth muscle in this region can be labeled with anti-SMA, anti-MLCK, and anti-SM22α, and also with nitric oxide indicators such as DAF-2DA. In other teleost species such as

Fig. 2. Confirmation of a smooth muscle-myocardium overlap in lungfish species. African (slender) lungfish *Protopterus dolloi* (A) and South American lungish *Lepidosiren paradoxa* (B) labeled with CH1 (myocardium—red) and SM22α (green). Cell nuclei are labeled with DAPI (blue). In each image, cranial is to the top. The smooth muscle of the outflow tract (OFT) extends to the base of the endocardial valves (arrowheads). The myocardial collar extends almost as far as the pericardial wall. Note however that a small portion of the distal OFT contains no myocardium. (C and D) Elastic trichrome stain of *Lepidosiren paradoxa* (B) and the Australian lungfish *Neoceratodus forsteri*. Note that similar to in the zebrafish, elastic and fibrous proteins (stained black) coincide with the smooth muscle cells almost to the proximal limit of the valves (arrowheads). Black arrows in (D) show the distal intrapericardial limit of the conal myocardium. AVP, atrioventricular plug. Scale bars = 1 mm.

Fig. 3. Chondrichthyans exhibit similar arterial pole architechture. (A) Sagittal section through the heart of *Dalatias licha*. Scale bar = 5 mm. Cranial to the top, dorsal to the left—elastic trichrome stains muscle brown, collagen red, and elastic proteins black. Abundant elastic fibers in the distal smooth muscle component of the outflow tract (OFT) extend caudally into the subendocardium as far as the most proximal valve leaflets. (A′) Detail of the ventral portion of the OFT marked by the dashed lines, labeled with anti-SM22α (green). Scale bar = 1 mm. Arrowheads show that smooth muscle is coincident with elastic fibers in the subendocardial layer. Autofluorescence in the myocardium has been artificially enhanced. (B) Longitudinal section through the OFT of *Etmopterus spinax*—elastic trichrome. Scale bar = 500 μm. Subendocardial elastic fibers (arrowheads) extend to the level of the most proximal valve leaflets. (B′) Detail of the region marked by dashed lines in (B). Anti-SMA shows coincident subendocardial smooth muscle (arrowheads) in *E. spinax*. Scale bar = 250 μm. Smooth muscle (arrowheads) extends to the most proximal valve. (C and D) The OFT of two *Galeus* spp., *G. atlanticus*, and *G. melastomus*, labeled with CH1 (red) and SM22α (green). Scale bars = 1 mm. Smooth muscle (arrowheads) extends to the most distal valves. (E) Detail of the arterial pole of *Scyliorhinus canicula*. Scale bar = 500 μm. The dorsal wall of the conus is shown in sagittal section. CH1 (red) and anti-SMA (green). In this species, the overlapping region is not so extensive, barely reaching the most distal valves (arrowheads). (F) Smooth muscle (arrowheads) extends beyond the distal valves in *Leucoraja naevus*. CH1 (red), SM22α (green). Scale bar = 250 μm. (G) Sagittal section of the heart of *Chimaera monstrosa*—CH1 (red), SM22α (green). Scale bar = 500 μm. Inset shows detail of the ventral OFT wall and that smooth muscle extends to the most proximal valves (arrowheads). Scale bar = 250 μm. A, atrium; DC, distal smooth muscle component (bulbus arteriosus); PC, proximal myocardial component (conus arteriosus); V, ventricle.

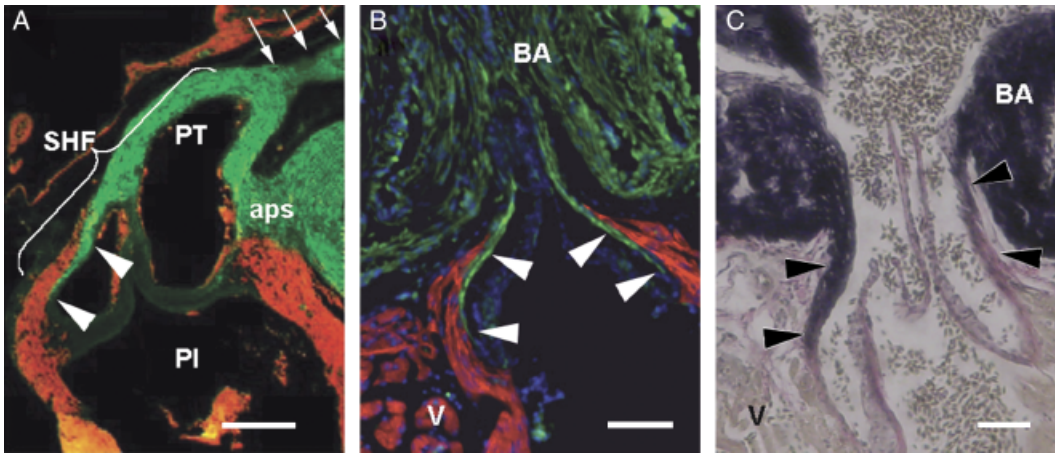
A
SHF
PT
aps
PI
B
BA
V
C
BA
V

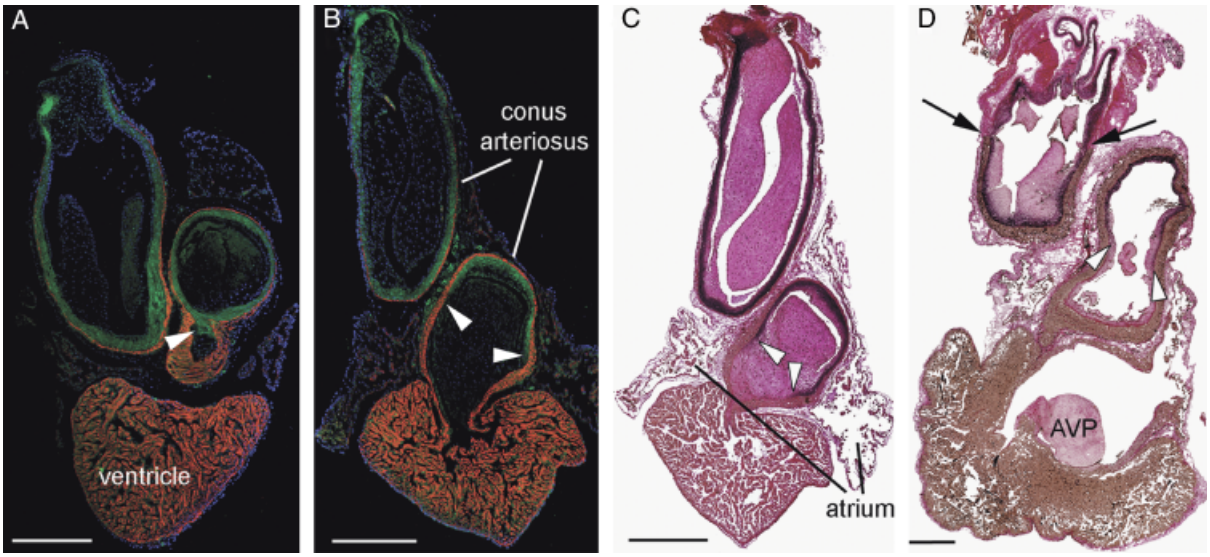
A
ventricle
B
conus
arteriosus
C
atrium
D
AVP

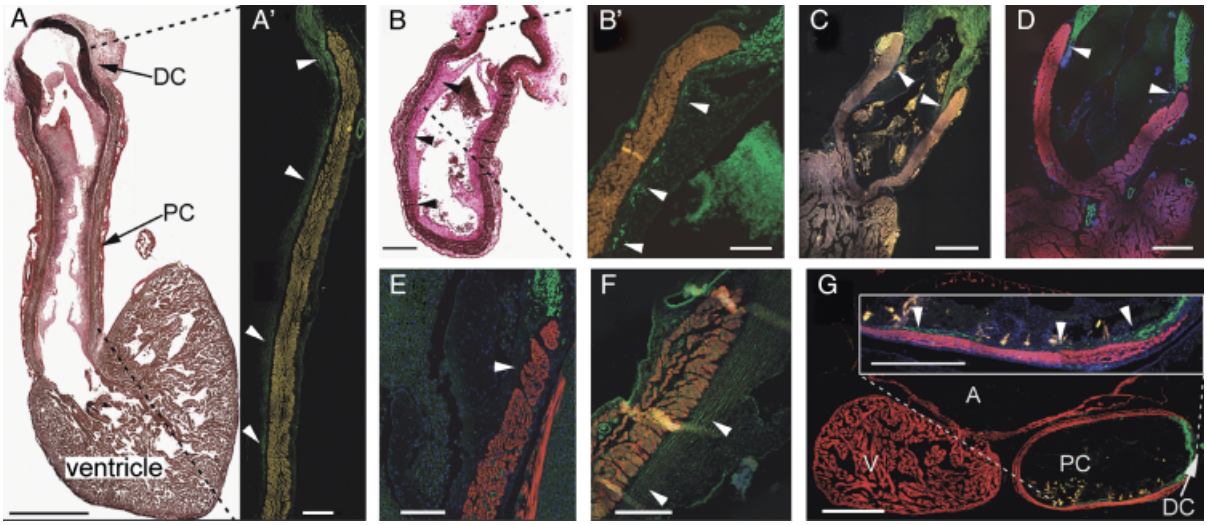
A
DC
PC
ventricle
A'
B
B'
C
D
E
F
G
A
V
PC
DC

the gilthead seabream *Sparus auratus*, the tissue that connects the myocardial conus arteriosus with the smooth muscle bulbus arteriosus has been described as a "fibrous ring" (Icardo et al. 2003) as it stains strongly with histochemical dyes for elastic and fibrous extracellular matrix proteins (Fig. 1C). However, we have confirmed that this tissue also possesses a smooth muscle phenotype by utilization of the several IHC markers listed above (Fig. 1B and data not shown).

One species for which a myocardial-smooth muscle overlap has previously been described is the African (slender) lungfish *Protopterus dolloi* (Icardo et al. 2005). In that report, the smooth muscle was identified by microscopic observation on semithin sections stained with Toluidine blue. Here we confirm, using an IHC approach, that such an overlap exists in *P. dolloi* and in representatives of the two other extant families of dipnoi (of which there are a total of six species), the South American lungfish *Lepidosiren paradoxa* and the Australian lungfish *Neoceratodus forsteri* (Fig. 2 and data not shown). Early descriptions of the OFT of lungfishes proposed that only the first (proximal) one-third portion of its length possessed a thick myocardial wall; the remaining two-thirds being "arterial-like" (e.g., Burggren and Johansen 1986). However, Icardo et al. (2005) described a thin myocardial sheath covering the entire length of the intrapericardial OFT. Our observations support that the OFT of three species of lungfishes possesses a thick myocardial wall for the proximal portion and a myocardial sheath over much of the remaining two-thirds of its length. However, the myocardium does not continue all the way to the junction of the pericardial cavity but rather terminates just short of the pericardial wall such that the last small portion contains only smooth muscle in its walls. This can be seen most obviously in the Australian lungfish (Fig. 2D). Thus, the most distal portion of the lungfish OFT is likely akin to the intrapericardial arterial trunk of more apical vertebrates such as avians and mammals.

Further to confirming the previously reported smooth muscle-myocardium overlap in zebrafish and lungfish, using the panel of antibodies and other histological techniques, we found a similar architecture at the arterial pole of all vertebrates studied. Although apparently ubiquitous, the extent and observability of this overlapping architecture was dependent upon each species and upon developmental stage.

Chondrichthyans

In some species of the most basal vertebrates, the chondrichthyans, it was not possible to label the tissue with the IHC markers available and we were unable to determine if this was due to the fixation processes or because the specific antigenic epitopes were not conserved. For example, neither myocardium nor smooth muscle could be effectively labeled in both species of torpediniformes acquired (*Torpedo nobiliana* and *Torpedo marmorata*) and whereas smooth muscle was labeled in *Dalatias licha* using SM22α, the myocardium was not adequately labeled by either MF20 or CH1. In such cases, we used normal histochemistry to show the presence of elastic fibers (that in zebrafish and lungfish are coincident with smooth muscle cells) and interpreted the data based on comparisons with species that were successfully labeled by IHC. Figure 3 shows arterial pole architecture in six species of chondrichthyan and highlights the myocardial-smooth muscle interface. In each case, the smooth muscle in this region was continuous with that of the most distal component of the OFT (the bulbus arteriosus—see Durán et al. 2008), and the myocardial conus arteriosus formed a collar around it, such that the overlapping architecture was evident most usually as far as the most distal outflow valves. In some elasmobranch species, in *Dalatias licha* and *Etmopterus spinax*, for example, some smooth muscle cells could be seen extending caudally as far as the most proximal outflow valves (Fig. 3, A′, B′, and C). We investigated one species of the chondrichthyan subclass holocephali, *Chimaera monstrosa*, and in this species, the myocardial-smooth muscle overlap also extended caudally beyond the most distal outflow valves (Fig. 3G). In contrast, in some elasmobranch species such as *Scyliorhinus canicula*, for example, the smooth muscle did not penetrate the sub-

Fig. 5. Basal actinopterygians. In all panels showing immunofluorescence, myocardium is labeled with CH1 (red) and, unless otherwise stated, smooth muscle is labeled with anti-SM22α (green). (A) Longitudinal section through the heart of the bichir *Polypterus senegalus*. Elastic stain shows abundant elastic fibers extending from the distal smooth muscle component (DC) of the outflow tract (OFT) deep into the subendocardium of the proximal component (PC). Scale bar = 1 mm. (B) Consecutive section of *P. senegalus*, anti-SMA (green) and DAPI (blue). Scale bar = 1 mm. (B′) Detail of the transition between proximal and distal OFT components showing myocardium-smooth muscle overlap. Scale bar = 100 μm. CV, coronary vessel, also labeled with anti-SMA. (B″) Detail of one lateral wall of the proximal OFT component of *P. senegalus*. Scale bar = 100 μm. Dashed line from (B) illustrates approximate relative position of the two sections. Note that the myocardium is also labeled with anti-SM22α, resulting in yellow fluorescence (see "Discussion"). White arrowheads show abundant smooth muscle cells in the subendocardial space. (C and D) Detail of the transition between proximal and distal OFT components of the sturgeons *Acipenser stellatus* and *Acipenser baeri*, respectively. Scale bars = 500 μm. (E) The OFT of the American paddlefish *Polyodon spathula*. Scale bar = 200 μm. Anti-SMA (green) highlights smooth muscle in the subendocardium (arrowheads). (F) The OFT of the bowfin *Amia calva*. Scale bar = 1 mm. Elastic stain shows elastic fibers deep within the subendocardium (arrowheads). Black arrows show the distal limit of the myocardial OFT component. (G) The heart of *Lepisosteus osseus*—elastic staining. Scale bar = 500 μm. A, atrium; DC, distal smooth muscle component (bulbus arteriosus); PC, proximal myocardial component (conus arteriosus); V, ventricle. (G′) Detail of the transition between proximal and distal OFT components of *L. osseus*. Scale bar = 150 μm. (G″) Detail of *L. osseus* proximal component wall. Dashed line from (G) shows approximate relative position of the two sections. Scale bar = 150 μm.

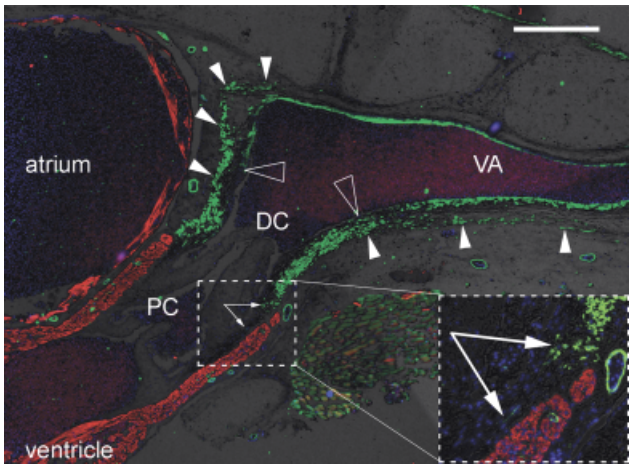

Fig. 4. Distinct origin of smooth muscle in distal OFT and ventral aorta? Sagittal section through the heart, outflow tract (OFT) and ventral aorta of a juvenile small-spotted catshark *Scyliorhinus canicula*, labeled with anti-SMA (green), CH1 (red), and DAPI (blue). Brightfield background shows gross tissue structure. Dorsal to the top, cranial to the right. Large hollow arrowheads show the distal limit of the intrapericardial OFT smooth muscle and, more cranially, the termination of most of the smooth muscle in the tunica media of the ventral aorta. Small arrowheads show where the OFT smooth muscle is continuous with smooth muscle in the pericardium/body wall (most obvious dorsally). Arrows in inset show smooth muscle cells in the subendocardium of the conus arteriosus. Scale bar = 500 μm. DC, distal smooth muscle component (bulbus arteriosus); PC, proximal myocardial component (conus arteriosus); VA, ventral aorta.

endocardium much further that the distal limit of the myocardium, such that the overlap was present, but minimal (Fig. 4). We were unable to establish any particular pattern of behavior, activity, or life-style that would indicate why some chondrichthyans may have a greater proportion and deeper caudal penetration of smooth muscle in the lumen of the OFT.

In several species examined (e.g., *Scyliorhinus canicula* and *Galeus melastomus*), the smooth muscle of the distal OFT component appeared to be anatomically distinct from the ventral aorta, such that a border could be identified at the cranial limit of the pericardial cavity (Fig. 4). Moreover, this population of distal OFT cells extended into the walls of the pericardial cavity.

Basal actinopterygians

The OFT of basal actinopterygians is similar to that of the chondrichthyans in that a prominent myocardial component persists into adulthood. We found a myocardial-smooth muscle overlap at the arterial pole of the spotted gar, two species of bichir, four species of sturgeon and the American paddlefish (likely the only surviving species of this family, as no Chinese paddlefish has been seen for over 3 years, suggesting that it may have already become extinct—Zhang et al. 2009). Figure 5 illustrates the OFT architecture of six representative nonteleost actinopterygians.

We noted that the myocardium in the OFT of the polypterid species *Polypterus senegalus* and *Polypterus ornatipinnis* labels with both the myocardial marker CH1 and also with the early marker for smooth muscle differentiation anti-SM22α (Fig. 5B″). Ventricular and atrial myocardium was not labeled by this marker.

We also obtained a number of young-of-year specimens of the bowfin *Amia calva*, a species limited to mainland United States. We were unable to label the tissues with IHC even after attempting several methods of antigen retrieval, probably due to the length of fixation (several years). Alternatively,

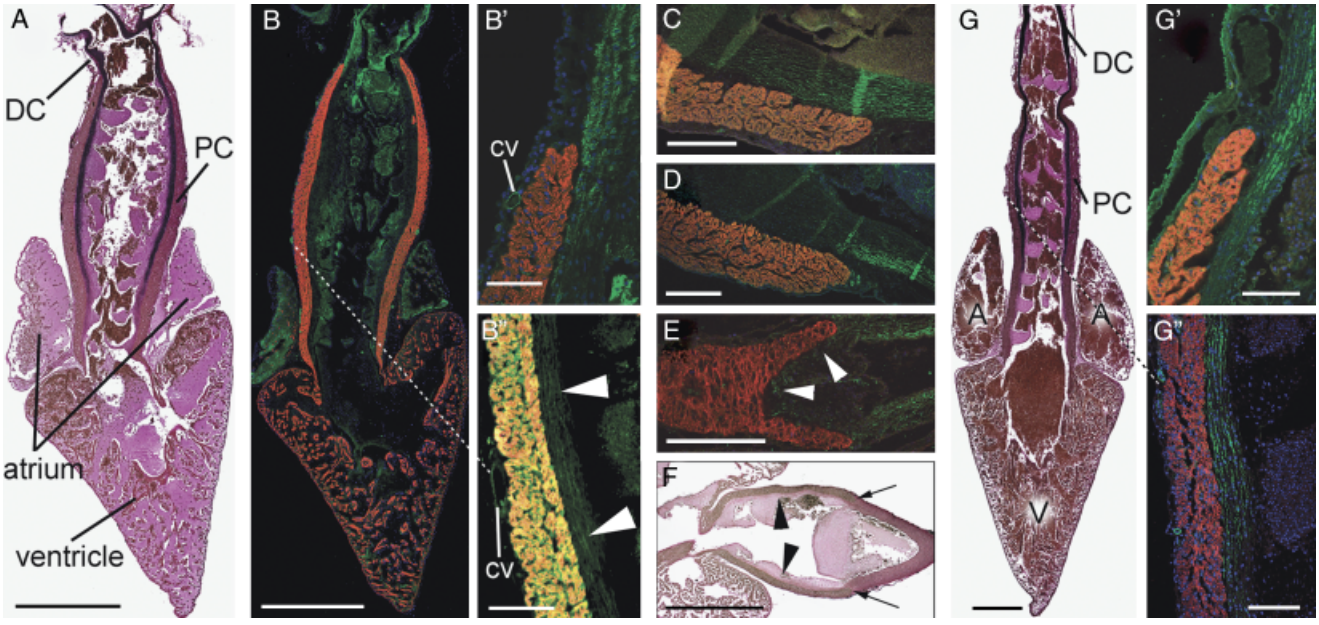

because it has been shown that the nascent smooth muscle of the bulbus arteriosus of zebrafish does not express markers of differentiation until very late in development (3 weeks post-fertilization—Grimes et al. 2006), it is also possible that these "young-of-year" bowfin did not yet have fully differentiated smooth muscle in the distal OFT. However, the extracellular elastic fibers present in the OFT of all other species examined were also obvious in sections of the hearts of this species (Fig. 5F). It therefore seems likely that smooth muscle cells also extend into the subendocardial space of this species, coincident with the elastic fibers.

Teleosts

In many teleosts, the myocardial conus arteriosus appears to have regressed over evolutionary time and, as a consequence, several researchers have proposed that the structure is merely vestigial or that it has been entirely lost and replaced by the bulbus arteriosus, which is comprised primarily of smooth muscle, collagen, and elastic fibers. However, of the 20 species we investigated (from 17 families and 11 orders) a myocardial conus arteriosus was identifiable in all as a region of myocardium, surrounding and supporting the outflow valves, that was morphologically quite distinct from the spongiosa, or trabeculated myocardium, of the ventricle. In six of the 20 species (*Channa micropeltes*, *Sander vitreus*, *Osteoglossum bicirrhosum*, *Apteronotus albifrons*, *Ctenolucius hujeta*, and *Sardina pilchardus*—representatives from six different families), the conus arteriosus was quite prominent and could not be considered "vestigial" (Fig. 6, C, D, E, F, G, and J, respectively). Furthermore, in all cases, smooth muscle cells lined the inside, lumenal face of the conal myocardium to a greater or lesser extent, depending on the species, in many cases extending to the level of the base of the outflow valves (Fig. 6). The overlapping architecture in the arterial pole was confirmed in most species examined using three different smooth muscle-specific antibodies.

The possibility of active cardiac valves in several vertebrate species has been discussed previously (e.g., Bushnell et al. 1992; Jones et al. 1993; Williams and Jew 2004; Muresian et al. 2006; Butcher and Markwald 2007). It was therefore noteworthy that in several species, including *Osteoglossum bicirrhosum*, *Channa micropeltes*, *Morone Chrysops*, and *Sardina pilchardus*, smooth muscle cells could be seen in the base of the outflow valves (Fig. 7—see also white arrowheads in Fig. 6E). We also noted that the valve sinuses of species such as *Scomber scrombrus* contained a considerable myocardial component (Fig. 7F).

In sagittal sections of *Menidia menidia* (Fig. 8), we observed coincident expression of both myocardial (CH1) and smooth muscle (SM22α) markers in the conus arteriosus and the atrioventricular canal (AVC), regions of the heart that in adulthood maintain a primary myocardial phenotype (i.e., nontrabeculated). The fact that this was only observed in one species of teleost is likely because most of our specimens were sectioned in a longitudinal orientation and, therefore, the OFT and AVC were not usually present in the same sections.

Tetrapods

An overlapping region of smooth muscle and myocardium is evident at the arterial pole of the chicken heart in late development (Waldo et al. 2005). We confirmed these results in chicken and found an equivalent overlap at a similar developmental stage in the duck heart (Fig. 9, C and D). Similar overlapping architecture was observed in four other tetrapod species (Fig. 9, A, B, and E). In the adult frog, smooth muscle can be seen overlapping the distal-most myocardium and in regions where the spiral valve makes contact with the myocardial wall of the OFT (Fig. 9A and data not shown). This observation has been presented in previous research, although not discussed in detail (e.g., Sedmera et al. 2003). In the green anole, overlapping smooth muscle and myocardium can be seen in both pulmonary and aortic outflows (Fig. 9B). In the case of the mouse the overlapping architecture is clearly visible at stages of development just after septation of the OFT has occurred (approximately E12.5) and is still evident at later fetal stages (Fig. 9E). However, as development proceeds, the OFT myocardium regresses toward the ventricle and the junction of myocardium with smooth muscle becomes more heavily invested with extracellular matrix and connective tissue containing abundant elastin and collagen (data not shown). Thus, although an overlapping architecture is seen during late developmental stages, it is much less clear postnatally.

As with some basal actinopterygians, the myocardial portion of the OFT of the adult frog also colabeled with CH1 and anti-SM22α, although not with anti-SMA (Fig. 10).

DISCUSSION

We have presented here a comprehensive analysis of the cardiac OFT of a wide range of vertebrate species. We have taken care to include representatives from as many groups as

Fig. 7. Smooth muscle and myocardium in the valve sinuses: evidence of active valving? (A–E) Five examples of teleost fish species with smooth muscle (labeled by anti-SM22α—green) in the base of the outflow valve (solid arrowheads). Myocardium is labeled by either MF20 or CH1 (red). (A) *Osteoglossum bicirrhosum*. (B) *Channa Micropeltes*. (C) *Sardina pilchardus*. (D) *Morone chrysops*. (E) *Morone americana*. (F) In *Scomber scombrus*, CH1 labeling (red) shows myocardium in the base of the valve (hollow arrowheads). DC, distal outflow tract component (bulbus arteriosus); PC, proximal outflow tract component (conus arteriosus). Scale bars = 250 μm.

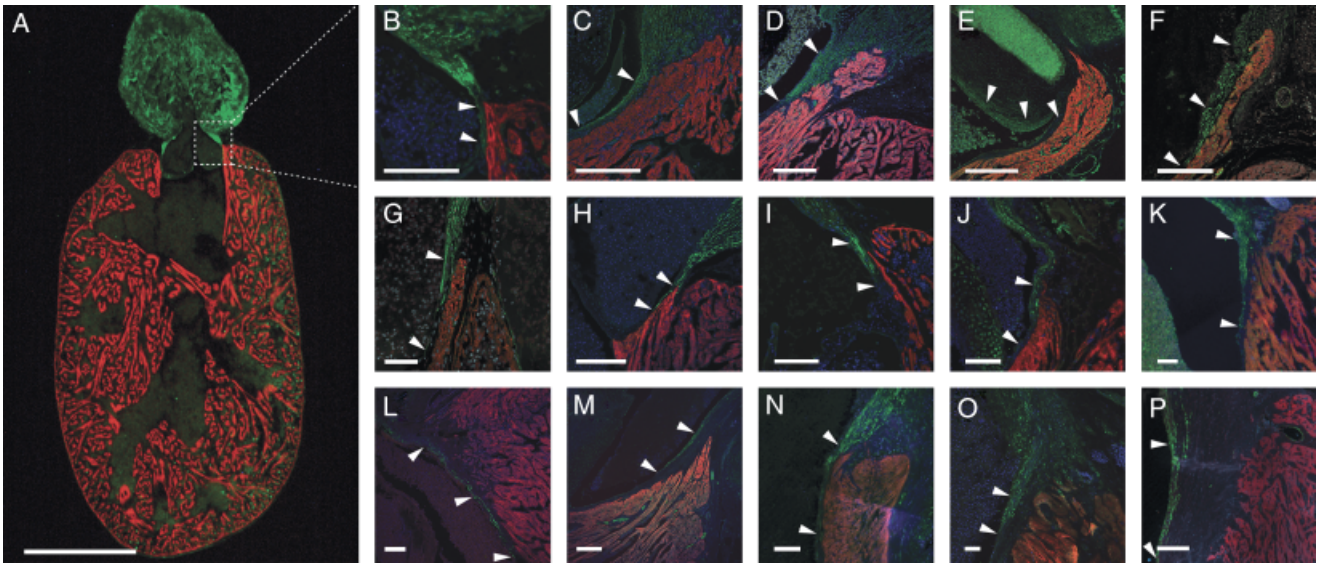

Fig. 6. Myocardial—smooth muscle overlap in the teleost arterial pole. (A) Longitudinal section through the heart of *Xiphophorus helleri*, a representative teleost, labeled with CH1 (red) and anti-MLCK (green). Cranial to the top. Scale bar = 500 μm. (B) Detail of one side of the arterial pole (boxed section in A) showing smooth muscle extending caudally into the myocardial region supporting the outflow valves (the conus arteriosus). Scale bar = 100 μm. (C–P) Details of similar regions in the arterial pole of 14 representative teleost species. Scale bars = 100 μm. Giant snakehead *Channa micropeltes* (C), walleye *Sander vitreus* (D), silver arowana *Osteoglossum bicirrhosum* (E), black ghost knife fish *Apteronotus albifrons* (F), gar characin *Ctenolucius hujeta* (G), Altlantic silverside *Menidia menidia* (H), suckermouth catfish *Hypostomus plecostomus* (I), European pilchard *Sardina pilchardus* (J), sea trout *Salmo trucha* (K), Atlantic mackerel *Scomber scombrus* (L), white bass *Morone chrysops* (M), large mouth bass *Micropterus salmoides* (N), gilthead seabream *Sparus auratus* (O), and skipjack tuna *Katsuwonus pelamis* (P). All are labeled with either CH1 or MF20 (red) and either anti-SMA, anti-MLCK, or anti-SM22α (green). DAPI (blue) labels nuclei. Arrowheads in each image show the overlapping region of overlap with smooth muscle and myocardium.

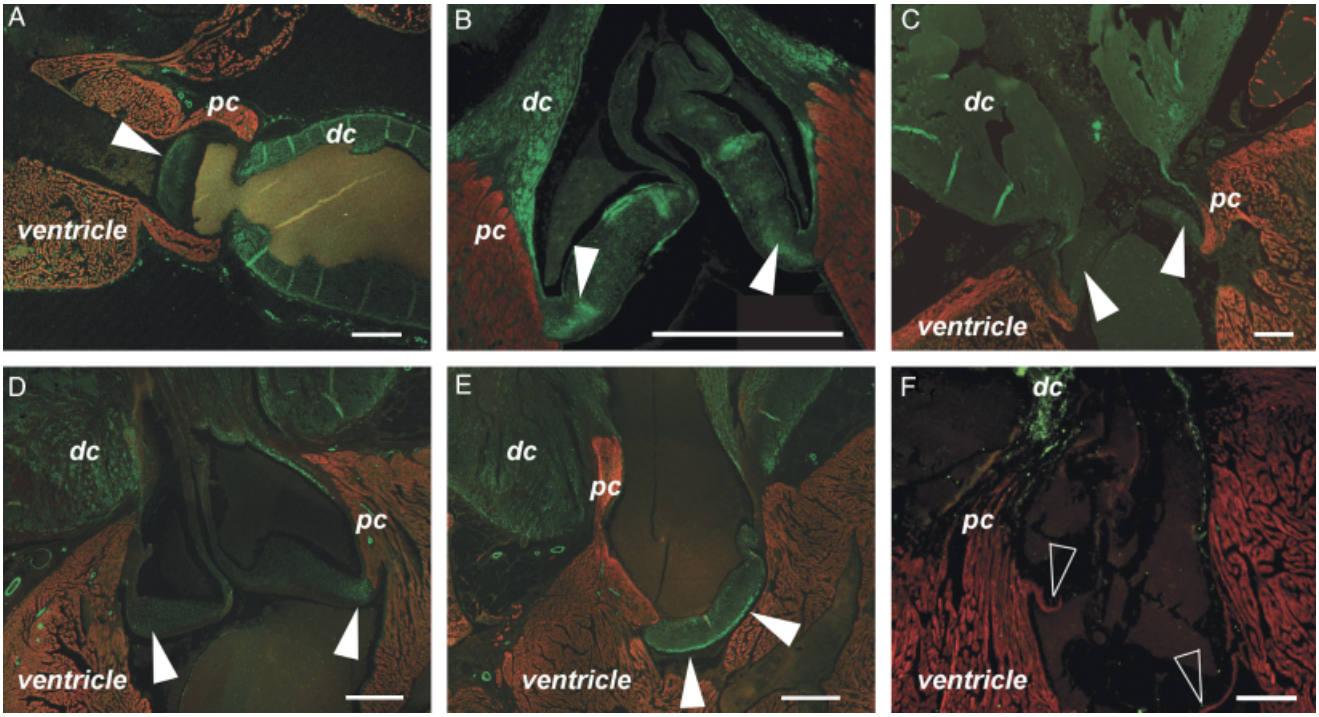

possible, especially among piscine species. The study includes 48 different species from 37 families and 27 orders. Based on these data, we suggest that the OFT of all vertebrates consists of three distinct components: a proximal, myocardial component that extends from the ventricular outflow to the base of the outflow valves; a distal, smooth muscle component extending from the cranial limit of the myocardial component to the wall of the pericardial cavity; and a middle component forming an overlapping seam between the proximal, myocardial and distal, smooth muscle OFT components.

Although smooth muscle has previously been described in the OFT subendocardial wall of several species, including the leopard shark (Yamauchi 1980), the chick (Waldo et al. 2005), the zebrafish, and the angular roughshark (Grimes and Kirby 2009) and, most recently, in the longnose gar (Zaccone et al. 2010), in a few other descriptions of the OFT of adult fishes, a population of cells residing in the subendocardium (i.e., at the lumenal side of the myocardial conus) has been identified as myofibroblasts, rather than smooth muscle (Hamlett et al. 1996; Icardo et al. 2002a, 2003). Under certain circumstances, including the responses to injury and disease, myofibroblasts are known to express "smooth muscle-specific" markers and, under such conditions, it may be difficult to distinguish them functionally, morphologically, or phenotypically from smooth muscle cells (Owens et al. 2004). However, whereas in the present study the existence of myofibroblasts has not been specifically addressed, the authors believe that in all cases presented the markers utilized are labeling primarily bona fide smooth muscle cells, because they comprise a limited population of cells at the myocardial-smooth muscle, arterial pole transition that are continuous with distal OFT cells *known* to possess a smooth muscle phenotype. For example, cells identified in the middle component of the OFT of some chondrichthyans generally constitute a relatively small subpopulation located at the myocardium-smooth muscle junction, whereas the myofibroblasts described in the aforementioned studies were in the context of tissue supporting the proximal valves (in the yellow spotted ray—Hamlett et al. 1996) or in the "conus valves and subendocardium" (in the sturgeon—Icardo et al. 2002a), rather than in the "conus-aorta transition" (Icardo et al. 2002b). Further, the myofibroblasts in previous studies were not identified by immunohistochemical techniques. Thus, while myofibroblasts are almost certainly present in the proximal subendocardial wall, it seems more parsimonious to assume that this limited population of cells, continuous as it is with the distal, smooth muscle OFT component and being labeled by markers such as anti-SMA, anti-TGLN, and anti-MLCK, is indeed smooth muscle.

It is important to note that in addition to smooth muscle, myocardium and myofibroblasts in the middle component of the OFT, there is a substantial presence of connective tissue and elastic fibers that is stained strongly with histochemical dyes for elastin and collagen. These fibers often stain strongly enough to make recognition of smooth muscle cells difficult (see Braun et al. 2003; Icardo et al. 2003). Moreover, in the postnatal mammalian heart, this connective tissue may be more abundant than smooth muscle and provides most of the material by which the proximal myocardium and distal smooth muscle are joined. It is only in early mammalian development that the overlapping architecture is obvious. Thus, when comparing the OFT of chondrichthyans and mammals, for example, the homologous structures and homologous architecture are most obvious in the embryo.

It is intriguing that an antibody raised against an early marker of smooth muscle differentiation, anti-SM22α, labels subpopulations of myocardial cells in some species. We noted such expression in the conus arteriosus of the frog (Fig. 10B) and several basal actinopterygians (Fig. 5), and also in the conus and AVC of at least one teleost species, the Atlantic silverside (Fig. 8), suggesting that the myocardium of the OFT possesses a distinct phenotype.

However, this phenomenon is not without precedent. As can be seen from Fig. 9E, the myocardium of the mouse heart expresses smooth muscle actin during embryonic development (see Sassoon et al. 1988) and this is known to occur in other species such as the rat (e.g., Ya et al. 1997) and chick (e.g., Ruzicka and Schwartz 1988; Sugi and Lough 1992). Such expression is gradually reduced in most of the myocardium during late development with a consequent increase in levels of sarcomeric actin isoforms, α-skeletal actin and α-cardiac actin. In the chick heart, the myocardium of the OFT and AVC maintains a smooth muscle phenotype until relatively late in development (Ruzicka and Schwartz 1988; Sugi and Lough 1992). This myocardium, and that of the "inner curvature" of the heart, is derived from the primary heart tube and thus ontogenetically "primitive." It is slow-conducting and has been described as "primary myocardium," thus distinguishing it from the fully differentiated "working" myocardium of the chambers (Moorman and Lamers 1994). However, it should be noted that not all of this myocardium is identical, there being a gradient of pacemaker activity along the tube, with the highest at the inflow (A. Moorman, personal communication). Also of note, relatively slow conduction velocities in the adult shark conus arteriosus (approximately 3 cm/sec, compared with approximately 50 cm/sec in the ventricle) have been proposed to support valve function (Teběcis 1967) and, although slower velocities are restricted to a narrow ring at the boundary between the ventricle and OFT in frogs (Irisawa et al. 1965), conus contraction is required for proper valve function in these animals (Johansen 1965; Langille and Jones 1977). It would be of great interest to determine whether our observation of persistent expression of a smooth muscle marker in the conus and AVC of the Atlantic silverside is evidence of pacemaker or nodal function in these regions of the teleost heart.

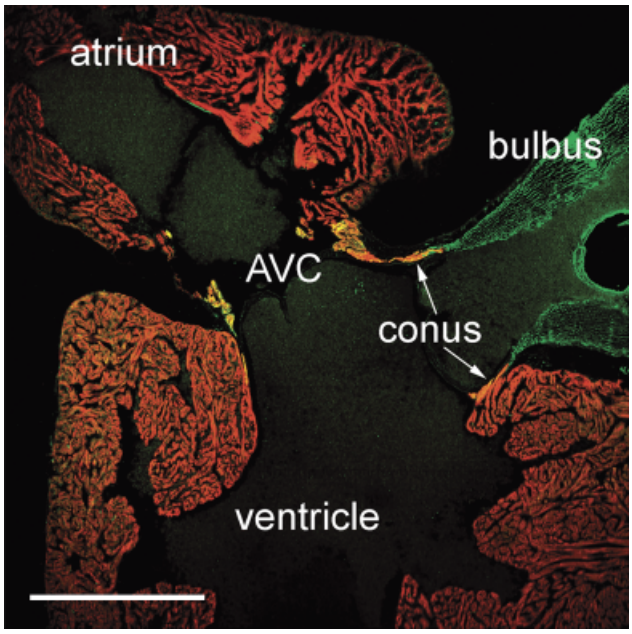

Fig. 8. "Primitive myocardium" in the conus arteriosus and atrioventricular canal of a teleost. Sagittal section of the Atlantic silverside (*Menidia menidia*) heart labeled with CH1 (red) and anti-SM22α (green). Myocardium in the conus arteriosus and in the atrioventricular canal (AVC) labels positively for both antibodies (see "Discussion"). Scale bar = 500 μm.

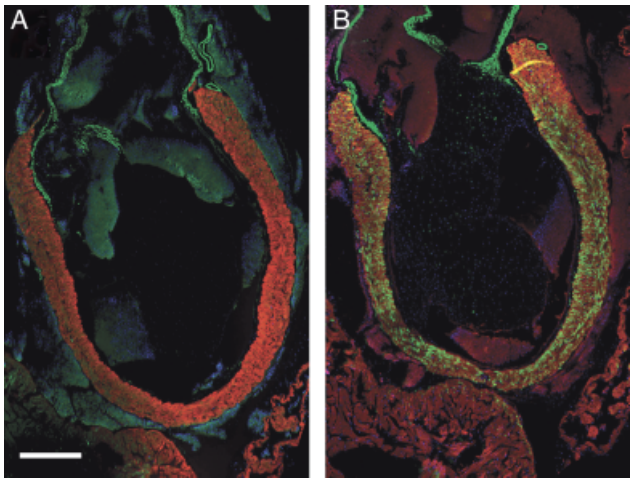

Fig. 10. *Xenopus* adult "primary myocardium" labels with anti-SM22α but not anti-SMA. (A) Longitudinal section through the outflow tract of *Xenopus*—DAPI, MF20 and anti-SMA. Scale bar = 500 μm. (B) Consecutive section labeled with DAPI, MF20, and anti-SM22α. The myocardium in the region of the outflow tract that supports the spiral valve labels with the smooth muscle marker (see "Discussion").

In contrast to SMA, based on expression patterns of LacZ in a trangenic mouse model, SM22α appears to be restricted to the myocardium of the primary heart tube in early development and then to the right ventricle and OFT from E11.5 (Li et al. 1996). Expression in this mouse is never seen in the left ventricle and disappears from all myocardium by E13.5. It has been proposed from a phylogenetic perspective that the right ventricle of hearts possessing four chambers may be derived from the conus arteriosus of more basal species such as the sharks and basal actinopterygians. Our observed persistent expression of SM22α in the conus arteriosus of bichirs and the frog appears to provide additional evidence for this notion and to our proposal that while ontogenetically the conus may be derived from the bulbus cordis (Goodrich 1930), phylogenetically the bulbus cordis may be derived from the conus.

Research has shown that a subpopulation of cells from a wider cardiogenic region (the heart field) of the vertebrate embryo adds to the heart late in development. This was originally demonstrated experimentally in chick and mouse—vertebrate models possessing a four-chambered heart. This

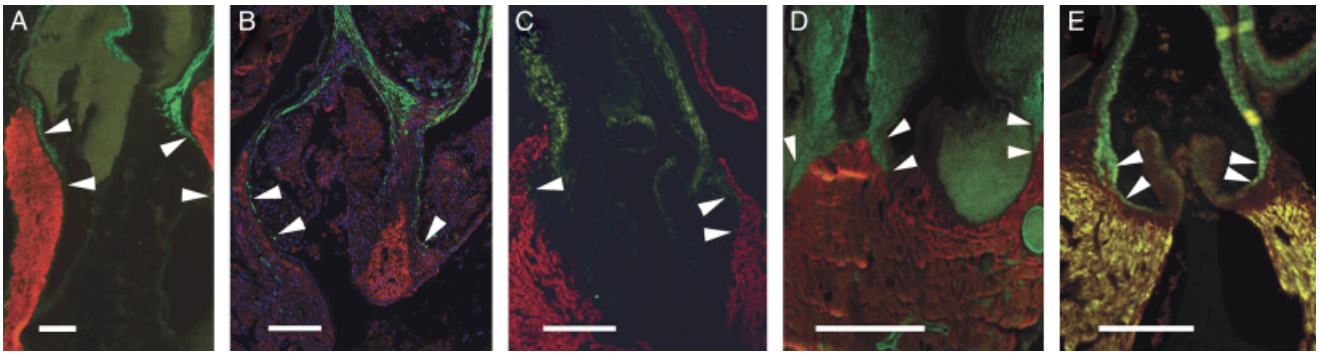

Fig. 9. Tetrapods. Myocardial to smooth muscle overlap (arrowheads) in five representative tetrapod species, labeled with MF20 (red) and anti-SMA (green), unless otherwise indicated. Scale bars = 250 μm. (A) Adult frog. Smooth muscle can be seen in regions where the spiral valve is in close contact with the myocardium. (B) Juvenile (10 cm) green anole. In this image, myocardium autofluorescence has been artificially enhanced and DAPI is blue. Smooth muscle can be seen extending caudally to the level of the valves on both pulmonary and aortic outflows. (C) Chick embryo (incubation day 11). See also Fig. 1A. (D) Duck embryo (incubation day 11). (E) Mouse embryo (E18.0). Note that mouse embryonic myocardium expresses SMA, hence yellow fluorescent signal.

population of cells from the cardiogenic mesoderm is described variously as the second, secondary or anterior heart field, depending on how the wider "primary heart field" is parsed (for reviews see Abu-Issa and Kirby 2007; Moorman et al. 2007). In this way, after formation of the heart tube, the heart continues to grow by proliferation of cells already present in the heart tube and, in part, by accretion of cells to both its venous and arterial pole from a proliferating growth center in the caudal coelomic wall (Soufan et al. 2006; van den Berg et al. 2009).

The secondary heart field (SHF) (as described by Waldo et al. 2005) is incorporated into the arterial pole, where a first "wave" of cells has been said to differentiate as myocardium, and a second wave as smooth muscle cells. However, because there is clearly an overlapping architecture in the arterial pole of all vertebrates studied here, it seems that the addition may not take the form of distinct waves, but rather as a continuum, where the majority of cells initially differentiate as myocardium, but, after a short developmental period, a few cells at the lumenal surface differentiate as smooth muscle. As development proceeds, and the OFT is extended, the ratio of lumenal smooth muscle to surrounding myocardium adjusts such that eventually all cells at the distal OFT differentiate as smooth muscle. Intriguingly, although it has been hypothesized in the past that the bulbus arteriosus of fishes may be derived from a "backward extension" of the ventral aorta (e.g., Lawson 1979), in several species examined here (e.g., *S. canicula* and *G. melastomus*) the smooth muscle of the distal OFT appears to be anatomically distinct from that of the ventral aorta, even in the adult, and extends into the pericardial wall. In contrast, while the endothelial lumen of the ventral aorta is continuous with the endocardium of the OFT, much of the smooth muscle of the tunica media terminates at the pericardial wall. This discontinuity suggests distinct origins of the two populations of smooth muscle cells. Based on these observations, it appears that a "SHF" may exist as a common theme in all vertebrates and that subtle changes in the programs of cell addition, differentiation (and perhaps proliferation) result in the wide phylogenetic variations observed in OFT morphology. Thus, in some groups, such as the chondrichthyans, there is a greater contribution of myocardial cells, which results in an extended conus arteriosus, whereas in most teleosts, especially in those belonging to phylogenetically apical taxa, there are greater numbers of cells which ultimately differentiate as smooth muscle, resulting in a much less substantial conus and an augmented bulbus arteriosus. In birds and mammals, an initial large contribution of myocardial cells undergoes remodelling processes such that much of it regresses toward and is incorporated into the ventricles, whereas a considerable smooth muscle contribution is being septated distally and augmented by cells from the neural crest (NC). The common theme we propose for the vertebrate OFT, then, is that its morphology varies gradually from proximal to distal such that the three components, or regions, described above can be identified: the proximal myocardial component, the distal smooth muscle component, and the middle component where myocardium and smooth muscle overlap. It is interesting to note as a generalization that the OFT valves are almost always supported by a collar of myocardium. It would be interesting to assess the mechanical advantage of this observation and, further, the structural advantage of having the junction of myocardium to smooth muscle being formed by overlap, rather than abutment.

A difficulty in the recognition or identification of the overlapping OFT architecture in the embryo of many species is that the cells of the OFT that will differentiate as smooth muscle do not label with immunohistochemical markers until relatively late in development. In the zebrafish, for example, markers such as anti-SMA and anti-MLCK are not effective in the OFT until approximately 3 weeks of development (Grimes et al. 2006). Similarly, in the chick, such markers do not label those cells of the OFT that are derived from the SHF until between HH stages 28–29 (approximately 6.5 days of fertilization), at which time the distal OFT has been septated by migrating NC cells (Waldo et al. 2005). Intriguingly, this SHF-derived population appears to be unique in this respect, as both NC-derived smooth muscle cells and those already present in the walls of the aortic sac, cells that do not contribute to the overlapping architecture, can be labeled with anti-SMA and anti-MLCK from considerably earlier in development (HH stage 22—approximately 3.5 days of fertilization). In contrast, as demonstrated in our previous work (Grimes et al. 2006; Durán et al. 2008; Grimes and Kirby 2009), *all* OFT smooth muscle, including the nascent smooth muscle of the chick and mouse SHF, and the proposed homologous OFT region of several other vertebrate species, can be labeled in vivo from much earlier in embryogenesis by nitric oxide indicators such as DAF-2DA. Further work with these compounds may shed light on the dynamics of the addition of cells to the OFT. One could speculate that the late phenotypic declaration of smooth muscle cells in the middle OFT component may result from the requirement by these cells to produce considerable quantities of extracellular matrix proteins to ensure a strong and elastic connection between myocardial and smooth muscle components of the OFT.

Since the initial description of secondary, second and anterior heart fields in chick and mouse, it has been an open question whether or not these developmental features exist in other, more basal species. But recent research has demonstrated that these fields are probably no more than regions of a wider "primary" cardiogenic field (see Abu-Issa and Kirby 2007; Moorman et al. 2007; Ma et al. 2008; Zhou and Pu 2008; Zhou et al. 2008), that are added relatively late in development after the dorsal mesocardium has detached from the body of the embryo and there are no alternative direct routes by which cells can add to the growing heart. The

different fields were identified primarily by their embryonic position at various stages of development and by their transient expression of genes such as *Islet1* and *Fgf10*, but their description as "distinct" heart fields is probably somewhat misleading. Cell tracing experiments in chick have demonstrated that there is a mediolateral, inflow-to-outflow organization of cardiac progenitor cells within the prefusion cardiogenic mesoderm (primary heart fields), such that cells closer to the midline are more likely to contribute to the OFT (Abu-Issa and Kirby 2007). Similarly, within the zebrafish lateral plate mesoderm it has been shown that ventricular progenitors are positioned closer to the midline than are cells that will form the atrium (Keegan et al. 2005). Recent work by de Pater et al. (2009) has also demonstrated that cells forming the myocardial portion of the zebrafish arterial pole are added to the heart between 34 and 48 hpf, and differentiate as myocardium later than those cells that form the initial heart tube, such that distinct phases of myocardial differentiation can be observed experimentally. All of these data suggest that the progenitors required for the late addition of tissue to the OFT are already present within the primary heart fields of both chick and zebrafish, and it is within those fields that the processes leading to the formation of the OFT are initiated. These secondary regions undoubtedly possess unique characteristics, not the least of which is the late declaration of phenotype by nascent smooth muscle cells that are incorporated into the middle OFT component. All vertebrates share similar processes of early cardiogenesis and form a heart tube by the migration to the midline and subsequent fusion of bilaterally paired cardiogenic fields. Thus, because the formation of a closed heart tube leaves only its inflow and outflow as routes by which cells can be added to the heart, it is perhaps unsurprising that similar "secondary" regions might exist as a common theme among vertebrates.

In a review of the formation of the ventricular OFTs, arterial valves and intrapericardial arterial trunks, Anderson et al. (2003) have discussed the controversial nature of embryonic OFT terminology and have suggested a simplified nomenclature of "proximal" and "distal" OFTs. Although these terms may describe different structures within different species, a simplified nomenclature may indeed be applicable and desirable across all vertebrates. The likely existence of *three* OFT components allows us to affirm the utility of such a simplified nomenclature for the cardiac OFT of *adult* species and, thereby, eliminate many of the confusing terms that pervade the literature. There may still be some minor difficulties with such a nomenclature, particularly in any attempts to ascribe homology to structures that exist in phylogenetically distant species. Another problem is the difficulty in recognizing the middle component without applying histochemical and/or immunohistochemical techniques. Further, the distal to proximal length of the middle component can vary widely, even between closely related species. However, because the heart of extant chondrichthyans represents the most basal gnathastomate condition, we propose that Gegenbaur's (1866) proposed nomenclature of conus arteriosus and bulbus arteriosus for the two distinct *anatomical* components of the adult chondrichthyan OFT is perfectly adequate. Then, with the elimination of terms such as bulbus cordis (other than in the strictest mammalian context), and by the recognition of the three *morphological* components of the vertebrate OFT, it may be easier to identify structures, both embryonically and in the adult, that share homology across species.

Thus, for example, the teleost bulbus arteriosus (which does not exist in early development) can be deemed homologous to the bulbus arteriosus of the chondrichthyan and basal actinopterygian OFT and to the arterial trunk of birds and mammals (that also do not exist in early development and could be more simply described as the distal OFT). Further, the part of the myocardial OFT component that contains the spiral valve in amphibian species such as *Xenopus* and in the dipnoi (lungfishes) can be recognized as the middle OFT component as it contains both myocardium and smooth muscle in its walls.

Acknowledgments

Optical microscopy was conducted with the help of Dr. Christian Hellriegel at the Microscopy & Dynamic Imaging Unit of the CNIC (Centro Nacional de Investigaciones Cardiovasculares), Madrid, Spain. Thanks to Antoon Moorman for helpful advice and critical reading of the manuscript. Thanks also to Juan-Manuel González-Rosa for useful discussions about the acquired data and to Roisin Doohan for assistance with histology. We thank Dr. Luis Gil de Sola from the Spanish Institute of Oceanography (Fuengirola, Málaga) for his assistance with Mediterranean species collection and identification, and Cristina Rodríguez (University of Málaga) for her assistance with collection and preparation of chondrichthyan hearts. ACG would like to extend his gratitude to Dr. Jonathan McDearmid at the University of Leicester for providing bench space and reagents. Also, we strongly appreciate the efforts of Kyle Erwin (NC, USA), Daniel Gefroh (ND, USA), Drs. Jan J. Hoover and Steven G. George (MI, USA), Drs. James E. Garvey and Sara Tripp (IL, USA), Professor Jean Joss (Sydney, Australia), Dr. José Luis Gómez-Skarmeta (Sevilla, Spain), and Nathan Honey (Cambridge, UK) for making our list of species much more comprehensive. AC Grimes & M Torres (CNIC) are funded by the Spanish Ministry of Science and Innovation (Grants RD06/0010/0008 and BFU2009-08331/BMC), and by the Pro-CNIC Foundation. AC Durán & V Sans-Coma are supported by the Ministerio de Educación y Ciencia, Spain (Grant CGL2006-0693) and FEDER funds. D Hami is supported by the NIH (Grant R01HL084413: Principle Investigator—Margaret L. Kirby), MM Santoro is supported by a Career Developmental Award from HFSP and AIRC.

REFERENCES

Abu-Issa, R., and Kirby, M. L. 2007. Heart field: from Mesoderm to heart tube. *Annu. Rev. Cell Dev. Biol.* 23: 45–68.

Anderson, R. H., Webb, S., Brown, N. A., Lamers, W., and Moorman, A. 2003. Development of the heart: (3) formation of the ventricular outflow tracts, arterial valves, and intrapericardial arterial trunks. *Heart* 89: 1110–1118.

Anderson, R. H., Wilkinson, J. L., and Becker, A. E. 1978. The bulbus cordis—a misunderstood region of the developing human heart: its significance to the classification of congenital cardiac malformations. *Birth Defects Orig. Artic. Ser.* 14: 1–28.

Bartelings, M. M., and Gittenberger-de Groot, A. C. 1989. The outflow tract of the heart - embryologic and morphologic correlations. *Int. J. Cardiol.* 22: 289–300.

Blitz, I. L., Andelfinger, G., and Horb, M. E. 2006. Germ layers to organs: using *Xenopus* to study "later" development. *Semin. Cell Dev. Biol.* 17: 133–145.

Braun, M. H., Brill, R. W., Gosline, J. M., and Jones, D. R. 2003. Form and function of the bulbus arteriosus in yellowfin tuna (*Thunnus albacares*), bigeye tuna (*Thunnus obesus*) and blue marlin (*Makaira nigricans*): static properties. *J. Exp. Biol.* 206: 3311–3326.

Burggren, W. W., and Johansen, K. 1986. Circulation and respiration in Lungfishes (Dipnoi). *J. Morphol. Suppl.* 1: 217–236.

Bushnell, P. G., Jones, D. R., and Farrell, A. P. 1992. The arterial system. In W. S. Hoar, D. J. Randall, and A. P. Farrell (eds.). *Fish Physiology, Vol XII The Cardiovascular System, Part A*. Academic Press, San Diego, pp. 89–139.

Butcher, J. T., and Markwald, R. R. 2007. Valvulogenesis: the moving target. *Philos. Trans. R. Soc. Lond. B: Biol. Sci.* 362: 1489–1503.

de Pater, E., et al. 2009. Distinct phases of cardiomyocyte differentiation regulate growth of the zebrafish heart. *Development* 136: 1633–1641.

Durán, A. C., Fernández, B., Grimes, A. C., Rodríguez, C., Arqué, J. M., and Sans-Coma, V. 2008. Chondrichthyans have a bulbus arteriosus at the arterial pole of the heart: morphological and evolutionary implications. *J. Anat.* 213: 597–606.

Ekström, P., and Korf, H. W. 1986. Substance P-like-immunoreactive neurons in the photosensory pineal organ of the rainbow trout, *Salmo gairdneri* Richardson (Teleostei). *Cell Tissue Res.* 246: 359–364.

Farrell, A. P., and Jones, D. R. 1992. The heart. In W. S. Hoar, D. J. Randall, and A. P. Farrell (eds.). *Fish Physiology, Vol XII The Cardiovascular System, Part A*. Academic Press, San Diego, pp. 1–88.

Gegenbaur, C. 1866. Zur vergleichenden Anatomie des Herzens. *Jenaisch. Z. Naturw.* 2: 365–383.

Goodrich, E. S. 1930. *Studies on the Structure and Development of Vertebrates*. Macmillan, London.

Grimes, A. C., and Kirby, M. L. 2009. The cardiac outflow tract of fishes: anatomy genes and evolution. *J. Fish Biol.* 74: 983–1036.

Grimes, A. C., Stadt, H. A., Shepherd, I. T., and Kirby, M. L. 2006. Solving an enigma: arterial pole development in the zebrafish heart. *Dev. Biol.* 290: 265–276.

Guerrero, A., et al. 2004. Differentiation of the cardiac outflow tract components in alevins of the sturgeon *Acipenser naccarii* (Osteichthyes, Acipenseriformes): implications for heart evolution. *J. Morphol.* 260: 172–183.

Hamlett, W. C., Schwartz, F. J., Schmeinda, R., and Cuevas, E. 1996. Anatomy, histology, and development of the cardiac valvular system in elasmobranchs. *J. Exp. Zool.* 275: 83–94.

Holmes, E. B. 2005. A reconsideration of the phylogeny of the tetrapod heart. *J. Morphol.* 147: 209–228.

Horb, M. E., and Thomsen, G. H. 1999. Tbx5 is essential for heart development. *Development* 126: 1739–1751.

Icardo, J. M. 2006. Conus arteriosus of the teleost heart: dismissed, but not missed. *Anat. Rec. Part A: Discoveries Mol., Cellular, Evol. Biol.* 288: 900–908.

Icardo, J. M., Brunelli, E., Perrotta, I., Colvee, E., Wong, W. P., and Ip, Y. K. 2005. Ventricle and outflow tract of the African lungfish *Protopterus dolloi*. *J. Morphol.* 265: 43–51.

Icardo, J. M., Colvee, E., Cerra, M. C., and Tota, B. 2002a. Structure of the conus arteriosus of the sturgeon (*Acipenser naccarii*) heart. I: the conus valves and the subendocardium. *Anat. Rec.* 267: 17–27.

Icardo, J. M., Colvee, E., Cerra, M. C., and Tota, B. 2002b. The structure of the conus arteriosus of the sturgeon (*Acipenser naccarii*) heart: II. The myocardium, the subepicardium, and the conus-aorta transition. *Anat. Rec.* 268: 388–398.

Icardo, J. M., et al. 2003. The conus valves of the adult gilthead seabream (*Sparus auratus*). *J. Anat.* 202: 537–550.

Irisawa, H., Hama, K., and Irisawa, A. 1965. Mechanism of slow conduction at the Bulbo-ventricular junction. *Circ. Res.* 17: 1–10.

Johansen, K. 1965. Cardiovascular dynamics in fishes, amphibians and reptiles. *Ann. N. Y. Acad. Sci.* 127: 414–442.

Jones, D. R., Brill, R. W., and Bushnell, P. G. 1993. Ventricular and arterial dynamics of anaesthetised and swimming tuna. *J. Exp. Biol.* 182: 97–112.

Keegan, B. R., Feldman, J. L., Begemann, G., Ingham, P. W., and Yelon, D. 2005. Retinoic acid signaling restricts the cardiac progenitor pool. *Science* 307: 247–249.

Kirby, M. L., and Waldo, K. L. 1995. Neural crest and cardiovascular patterning. *Circ. Res.* 77: 211–215.

Laane, H. M. 1973a. The nomenclature of the arterial pole of the embryonic heart. I. Review of the literature up to 1750. *Acta Morphol. Neerlando-Scand.* 12: 167–176.

Laane, H. M. 1973b. The nomenclature of the arterial pole of the embryonic heart. II. Review of the literature from 1750–1890. *Acta Morphol. Neerlando-Scand.* 12: 177–184.

Laane, H. M. 1973c. The nomenclature of the arterial pole of the embryonic heart. III. Review of the literature from 1890–1973. *Acta Morphol. Neerlando-Scand.* 12: 185–194.

Laane, H. M. 1973d. The nomenclature of the arterial pole of the embryonic heart. IV. Discussion and conclusion. *Acta Morphol. Neerlando-Scand.* 12: 195–210.

Langille, B. L., and Jones, D. R. 1977. Dynamics of blood flow through the hearts and arterial systems of anuran amphibia. *J. Exp. Biol.* 68: 1–17.

Lawson, R. 1979. The comparative anatomy of the circulatory system. In M. H. Wake (ed.). *Hyman's Comparative Vertebrate Anatomy*. 3rd Ed. University of Chicago Press, Chicago, pp. 448–554.

Li, L., Miano, J. M., Mercer, B., and Olson, E. N. 1996. Expression of the *SM22a* promoter in transgenic mice provides evidence for distinct transcriptional regulatory programs in vascular and visceral smooth muscle cells. *J. Cell Biol.* 132: 849–859.

Ma, Q., Zhou, B., and Pu, W. T. 2008. Reassessment of Isl1 and Nkx2-5 cardiac fate maps using a Gata4-based reporter of Cre activity. *Dev. Biol.* 323: 98–104.

Moorman, A. F., Christoffels, V. M., Anderson, R. H., and van den Hoff, M. J. B. 2007. The heart forming fields: one or multiple? *Philos. Trans. R. Soc. B: Biol. Sci.* 362: 1257–1265.

Moorman, A. F., and Lamers, W. H. 1994. Molecular anatomy of the developing heart. *Trends Cardiovasc. Med.* 4: 257–264.

Muresian, H., Diena, M., Cerin, G., and Filipoiu, F. 2006. The mitral valve: new insights into the clinical anatomy. *Mædica* 1: 80–87.

Orts-Llorca, F., Puerta-Fonollá, J., and Sobrado, J. 1982. The formation, septation and fate of the truncus arteriosus in man. *J. Anat.* 134: 41–56.

Owens, G. K., Kumar, M. S., and Wamhoff, B. R. 2004. Molecular regulation of vascular smooth muscle cell differentiation in development and disease. *Physiol. Rev.* 84: 767–801.

Romer, A. S., and Parsons, T. S. 1986. *The Vertebrate Body*. Saunders College Publishing, Philadelphia.

Ruzicka, D. L., and Schwartz, R. J. 1988. Sequential activation during avian cardiogenesis: vascular smooth muscle α-actin gene transcripts mark the onset of cardiac differentiation. *J. Cell Biol.* 107: 2575–2585.

Santoro, M. M., Pesce, G., and Stainier, D. Y. 2009. Characterization of vascular mural cells during zebrafish development. *Mech. Dev.* 126: 638–649.

Sassoon, D. A., Garner, I., and Buckingham, ME. 1988. Transcripts of α-cardiac and α-skeletal actins are early markers for myogenesis in the mouse. *Development* 104: 155–164.

Satchell, G. H. 1991. *Physiology and Form of Fish Circulation*. Cambridge University Press, Cambridge.

Schib, J. L., et al. 2002. The conus arteriosus of the adult gilthead seabream (*Sparus auratus*). *J. Anat.* 201: 395–404.

Sedmera, D., et al. 2003. Functional and morphological evidence for a ventricular conduction system in zebrafish and Xenopus hearts. *Am. J. Physiol.—Heart Circ. Physiol.* 284: H1152–H1160.

Soufan, A. T., van den Berg, G., Ruijter, J. M., de Boer, P. A., van den Hoff, M. J., and Moorman, A. F. 2006. Regionalized sequence of myocardial cell growth and proliferation characterizes early chamber formation. *Circ. Res.* 99: 545–552.

Sugi, Y., and Lough, J. 1992. Onset of expression and regional deposition of alpha-smooth and sarcomeric actin during avian heart development. *Dev. Dyn.* 193: 116–124.

Teběcis, A. K. 1967. A study of electrograms recorded from the conus arteriosus of an elasmobranch heart. *Aust. J. Biol. Sci.* 20: 843–846.

Thompson, R. P., Sumida, H., Abercrombie, V., Satow, Y., Fitzharris, T. P., and Okamoto, N. 1985. Morphogenesis of human cardiac outflow. *Anat. Rec.* 213: 578–586.

van den Berg, G., et al. 2009. A caudal proliferating growth center contributes to both poles of the forming heart tube. *Circ. Res.* 104: 179–188.

Waldo, K. L., et al. 2005. Secondary heart field contributes myocardium and smooth muscle to the arterial pole of the developing heart. *Dev. Biol.* 281: 78–90.

Webb, S., Qayyum, S. R., Anderson, R. H., Lamers, W. H., and Richardson, M. K. 2003. Septation and separation within the outflow tract of the developing heart. *J. Anat.* 202: 327–342.

Williams, T. H., and Jew, J. Y. 2004. Is the mitral valve passive flap theory overstated? An active valve is hypothesized. *Med. Hypotheses* 62: 605–611.

Ya, J., Markman, M. W., Wagenaar, G. T., Blommaart, P. J., Moorman, A. F., and Lamers, W. H. 1997. Expression of the smooth-muscle proteins alpha-smooth-muscle actin and calponin, and of the intermediate filament protein desmin are parameters of cardiomyocyte maturation in the prenatal rat heart. *Anat. Rec.* 249: 495–505.

Yamauchi, A. 1980. Fine structure of the fish heart. In G. H. Bourne (ed.). *Hearts and Heartlike Organs*. Academic Press, New York, pp. 119–148.

Zaccone, D., et al. 2010. Complex innervation patterns of the conus arteriosus in the heart of the longnose gar, *Lepisosteus osseus*. *Acta Histochem.* (in press). doi: 10.1016/j.acthis.2010.06.004.

Zhang, H., Wei, Q. W., Du, H., Shen, L., Li, Y. H., and Zhao, Y. 2009. Is there evidence that the Chinese paddlefish (*Psephurus gladius*) still survives in the upper Yangtze River? Concerns inferred from hydroacoustic and capture surveys, 2006–2008. *J. Appl. Ichthyol.* 25: 95–99.

Zhang, Q., Li, Z., and Gui, J. 2001. *In vitro* culture of embryonic hearts from guppy fish (*Poecilia reticulata*). *Chin. Sci. Bull.* 46: 1638–1641.

Zhou, B., et al. 2008. Epicardial progenitors contribute to the cardiomyocyte lineage in the developing heart. *Nature* 454: 109–113.

Zhou, B., and Pu, W. T. 2008. More than a cover: epicardium as a novel source of cardiac progenitor cells. *Regenerative Med.* 3: 633–635.